Early diagenetic septarian concretions from the Oxfordian (Jurassic) Corallian Group, Osmington Mills, Dorset, UK

D. J. Green and D. Pirrie

Green, D.J. and Pirrie, D. 2001. Early diagenetic septarian concretions from the Oxfordian (Jurassic) Corallian Group, Osmington Mills, Dorset, UK. *Geoscience in south-west England*, **10**, 000-000.

Early diagenetic septarian concretions nucleated around large oyster shells are common in the Oxfordian (Late Jurassic) Nothe Grit Formation of the Corallian Group at Osmington Mills, Dorset, UK. The host sediment is dominated by quartz, feldspar, mica and clay minerals along with abundant bioclasts. The concretions are predominantly composed of non-ferroan calcite, post-dated by ferroan calcite, along with minor pyrite, glauconite and silica (chalcedony and quartz) cements. Radial septarian fractures are infilled by non-ferroan and ferroan calcite cements. The first phase of calcite cementation occurred prior to significant compaction; septarian fracture generation occurred following burial and localised over-pressuring of the sediment.

Camborne School of Mines, University of Exeter, Redruth, Cornwall, TR15 3SE, U.K.
(E-mail dpirrie@csm.ex.ac.uk).

Introduction

Early diagenetic carbonate concretions are a common feature in many sedimentary basins where they provide a record of changing fluid chemistry and cementation phases during shallow burial (e.g. Raiswell, 1971, 1987; Scotchman, 1993; Wilkinson, 1992, 1993). However, aspects of the mechanisms of concretion nucleation and growth are still poorly known. For example, some concretions contain radially or horizontally arranged carbonate-filled fractures or septaria, the formation of which is still controversial (e.g. Hounslow, 1997; Hudson *et al.,* 2001; Pratt, 2001). In this paper a detailed petrographic description of early diagenetic septarian concretions from the Nothe Grit Formation of the Corallian Group, Osmington Mills, Dorset is presented (Figure 1). Previous work on concretions from this area focussed on the large concretions (1 – 2 m diameter), which occur within the overlying Bencliff Grit Formation. Whilst the presence of concretions in the Nothe Grit Formation has been noted by previous workers (e.g. Arkell, 1936; Coe, 1995), there are no previously published petrographic descriptions of these concretions.

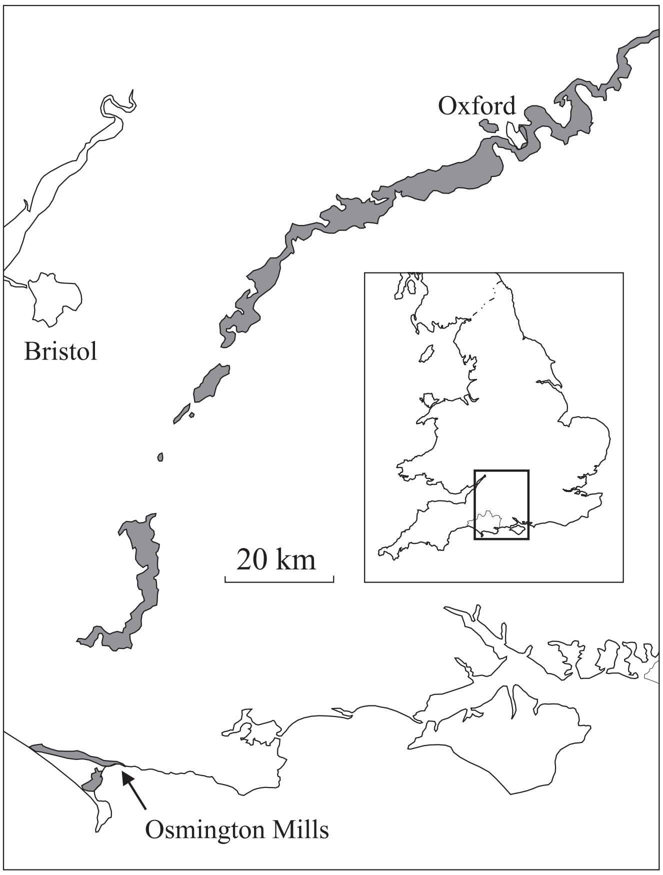

Figure 1. *Sketch map showing the outcrop of the Corallian Group in southern England and the location of Osmington Mills. Modified from Talbot (1973).*

Regional setting

The Oxfordian Corallian Group crops out along the Dorset coast in the area around Weymouth (Coe, 1995; Newell, 2000). It overlies the Oxford Clay Formation and is in turn overlain by the Kimmeridge Clay Formation (Coe, 1995) (Figure 2). The group comprises an alternating succession of mudstones, sandstones and limestones that show marked cyclicity interpreted to reflect repeated regressive-transgressive cycles linked to eustatic sea level change (Arkell, 1933; Wilson, 1968; Talbot, 1973; Sun, 1989, 1990). Four main transgressive-regressive cycles are recognised with deposition taking place on a storm and tidally-influenced shallow epicontinental shelf (Sun, 1990). Coe (1995) and Newell (2000) provide a sequence stratigraphic framework for the group, with the Nothe Grit Formation bounded both above and below by unconformities (see also Oxford *et al.*, 2000).

Previous diagenetic studies on the Corallian Group have either focussed upon concretions from the Bencliff Grit Formation (e.g. Walderhaug *et al.,* 1989; Bjorkum and Walderhaug, 1990) or have described the diagenesis of the overall succession (Wright, 1986; de Wet, 1987).

In this study concretions were examined from the Nothe Grit Formation which crops out in the cliff section and foreshore approximately 50 m to the east of the slipway at Osmington Mills, Dorset (Figure 1; SY 734 817). The cliff section exposes the upper part of the Nothe Grit Formation and the overlying Preston Grit Member of the Redcliff Formation (Figure 3). The Nothe Grit Formation is an intensely bioturbated muddy siltstone which generally coarsens up to a fine grained well sorted sandstone (Wright, 1986; Coe, 1995). The macrofauna present is dominated by the large oyster *Gryphaea dilatata* J. Sowerby 1818, along

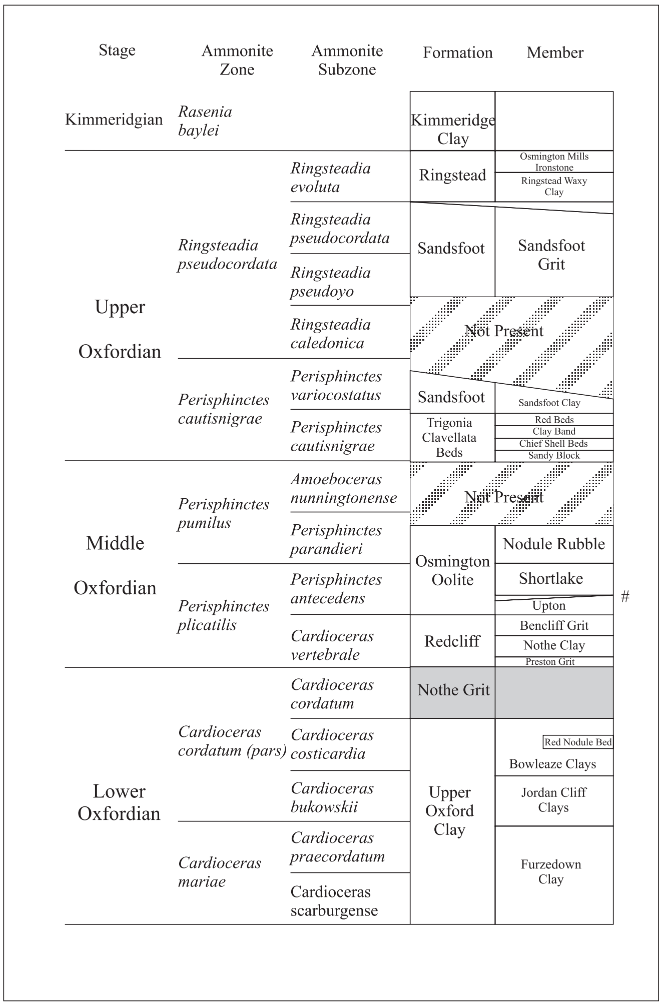

Figure 2. *Stratigraphy of the Corallian Group (after Coe, 1995). # indicates the presence of a minor unconformity at this level.*

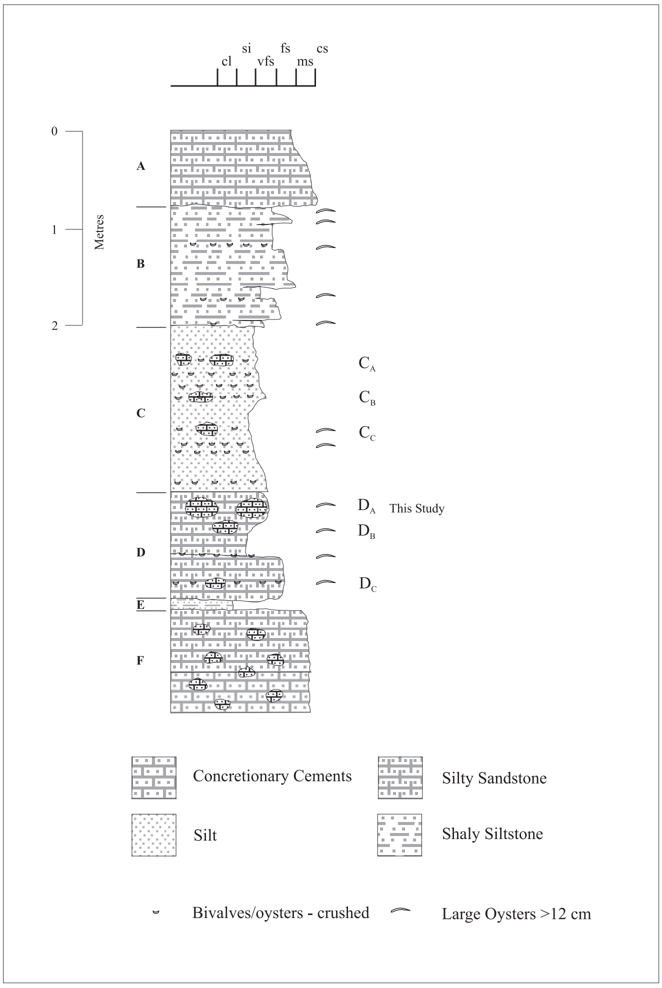

Figure 3. *Graphic sedimentary log for the section through the Nothe Grit Formation (B to F) and overlying Preston Grit Member (A), Osmington Mills. A to F are bed divisions, $C_{A\text{-}C}$ and $D_{A\text{-}C}$ and concretion-dominated beds.*

with smaller encrusting forms such as *Lopha gregaria*. Ammonites also occur but are rare and are usually preserved as moulds. The Nothe Grit Formation has been assigned to the Lower Oxfordian *Cardioceras cordatum* subzone (Coe, 1995).

Bed-parallel concretion horizons are present at a number of levels within the formation. In this study concretions from bed D_A which contains the largest concretions at this outcrop, were sampled (Figure 3). The concretions are up to 37 cm in diameter ranging in shape from oblate spheroids to more elongated forms which show no clear preferred orientation. In some cases the shape of the upper and lower surfaces of the concretion appears to mimic the shape of the large oysters which form their central nucleus. The sampled horizon is composed of intensely bioturbated silty sandstone; the intense bioturbation obscures any textural relationship between the concretions and the surrounding host sediment. However, the absence of any textural evidence for compaction in thin section implies that the concretions grew prior to significant compaction, i.e. are early diagenetic in origin (Dickson and Barber, 1976; Wolff *et al.*, 1992; Hesselbo and Palmer, 1992).

Methods

Two concretions were orientated in the field and then sampled. The concretions were serially sliced perpendicular to the horizontal plane and parallel to the N-S orientation, the resultant slabs being between 0.8 and 2 cm thick (Figure 4). All of the key features on each cut face were then traced (Figure 5) and digitised for 3D modelling of the concretion form. Fifty uncovered polished thin sections were prepared from both vertical and horizontal transects across three slabs from each concretion. The thin sections were examined under transmitted and reflected light microscopy (using a Nikon Labophot microscope) and cathodoluminescence (CL) (using a Technosyn cold cathode CL at 15 kV and gun currents of 400 - 450 mA), followed by carbonate staining using the methodology of Dickson (1966). Representative samples were also examined using a JEOL 840 scanning electron microscope (SEM) with an Oxford Instruments (Link System) AN10000 energy dispersive spectrometer (EDS). In addition samples of the surrounding host sediment were thin sectioned for comparison with the concretions.

Sample description

In the slabbed faces the concretions appear to have nucleated around large articulated oysters identified as *Gryphaea dilatata* J. Sowerby 1818 (Figure 4). The oysters are inverted and have formed a pseudo-hardground, or benthic island, with small encrusting oysters on the exterior of the upturned lower valve along with encrusting foraminifera. In addition both valves show prominent borings ranging in size between 1 cm and < 1 mm. The sediment surrounding the oyster shell sections is a poorly sorted silty sandstone showing intense bioturbation. Several discrete ichnogenera are present; Fürsich (1975) assigned these traces to the *Teichichnus* association which is dominated by sub-horizontal burrows interpreted to represent shallow burrowing deposit feeders in a stable subtidal substrate.

Prominent septarian fractures cross cut the oyster shells and radiate out towards the edge of the concretion (Figure 4). Brown calcite forms a fringe to the fractures and is postdated by yellow

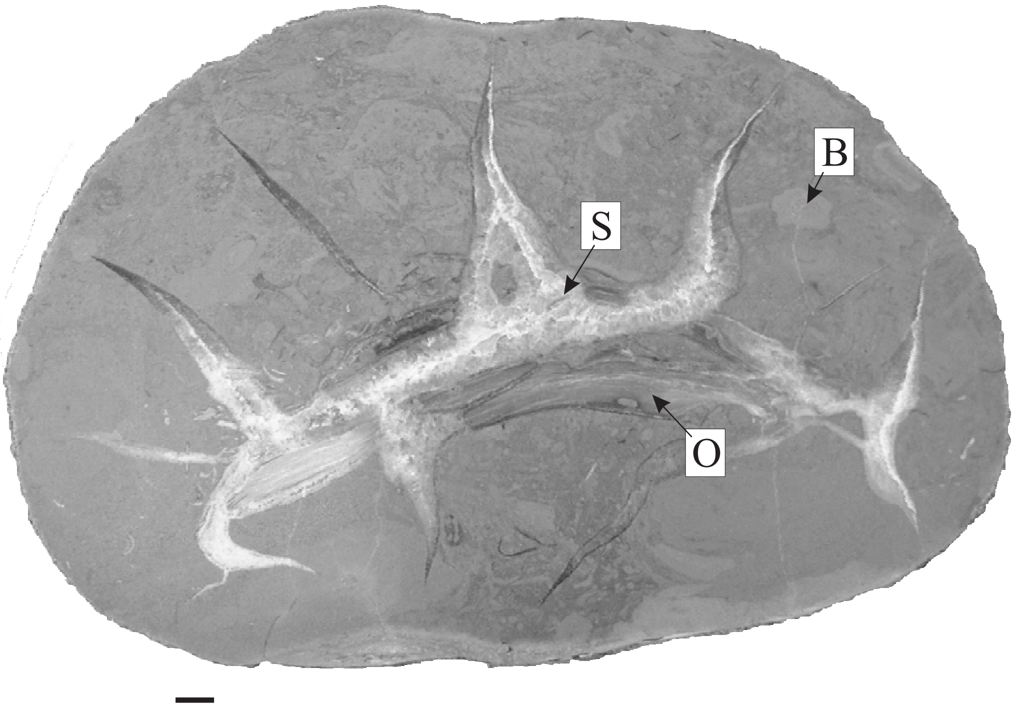

Figure 4. *Photograph showing features of a slabbed concretion oriented in the N-S plane. Visible are striking septarian fractures (S), oyster nucleus (O) and abundant burrows (B). Scale bar is 1 cm.*

and finally a clear calcite cement. The septarian fractures do not extend to the concretion rim, usually stopping about 1 cm from the edge, where they appear to be deflected to a position paralleling the concretion margin. The oyster shells show fractures both following the original lamellar ultrastructure and also cross-cutting the shell medially.

PETROGRAPHY

Host sediment

The mineralogy of the host sediment is dominated by quartz, clay and subordinate microcline feldspar and muscovite. Burrows are poorly defined and/or flattened and deformed; larger burrow forms are infilled by dark grey silty clay. Disarticulated and fragmented bivalve shells occur along with foraminifera (cf. Oxford *et al*., 2000). Some of the bivalve shells (mainly oysters) are partially replaced by quartz cements. Diagenetic phases present include pyrite which occurs both as infills in chambers of foraminifera and also disseminated throughout the sediment, along with both microspar and patchy poikilotopic calcite cements.

Concretion detrital mineralogy and bioclasts

The detrital mineralogy of the Nothe Grit Formation concretions is dominated by monocrystalline quartz along with minor polycrystalline undulose extinction quartz, muscovite, microcline and clay minerals. The quartz grains range from 20-250 μm in size (coarse silt to fine sand) predominantly in the range 60-90 μm (very fine sand) and are subangular with rare point contacts. Bioclasts are abundant including bivalves, foraminifera, echinoids, rare gastropods and wood fragments. The dominant bioclasts present are the large oysters *Gryphaea dilatata* J. Sowerby 1818 which form the concretion nucleus. The outer part of the oyster shells are dominated by non-ferroan, non-luminescent foliated calcite. This overlies an inner layer of non-luminescent, non-ferroan prismatic calcite. The foliated shell layer is commonly fractured parallel to the foliation with either ferroan or non-ferroan calcite and/or chalcedony cements infilling the fractures. The prismatic shell layer is also fractured, typically with alteration rimming the prisms.

In addition to the large oysters, other smaller oysters also occur, either encrusting the large forms or occurring as disarticulated valves composed of non-luminescent, non-ferroan foliated calcite, which is partially replaced by zoned ferroan calcite cements. Small (typically 1-2 mm) disarticulated and fragmented bivalve shells also occur disseminated throughout the concretions and are composed of either non-ferroan or ferroan calcite showing dull orange luminescence under CL. Small articulated bivalves with non-luminescent non-ferroan calcite shells are also common. No moulds of aragonitic shells were observed.

Many of the bivalve shells contain abundant macro- or microborings. The larger borings are up to 6 mm in diameter. The majority of them are infilled with non-ferroan calcite cement. Under CL the borings have a bright orange rim which is ferroan calcite, post-dated by dull orange luminescent non-ferroan calcite. A second set of borings are 500 μm in diameter and occur in thinner shells ($<$2 mm thick), and are infilled by either ferroan or non-ferroan calcite cement. Microborings are present at the rim of some large oysters, but are more common on thinner encrusting oysters and the other bivalves. The microborings are $<$100 μm across penetrating to 200 μm and with a bottle-shaped form.

Foraminifera are abundant throughout the concretions although they do appear concentrated within specific horizons. Taxa identified include *Nodosaria* sp. and *Lenticulina* sp., the latter genus being the most common along with rare milioline

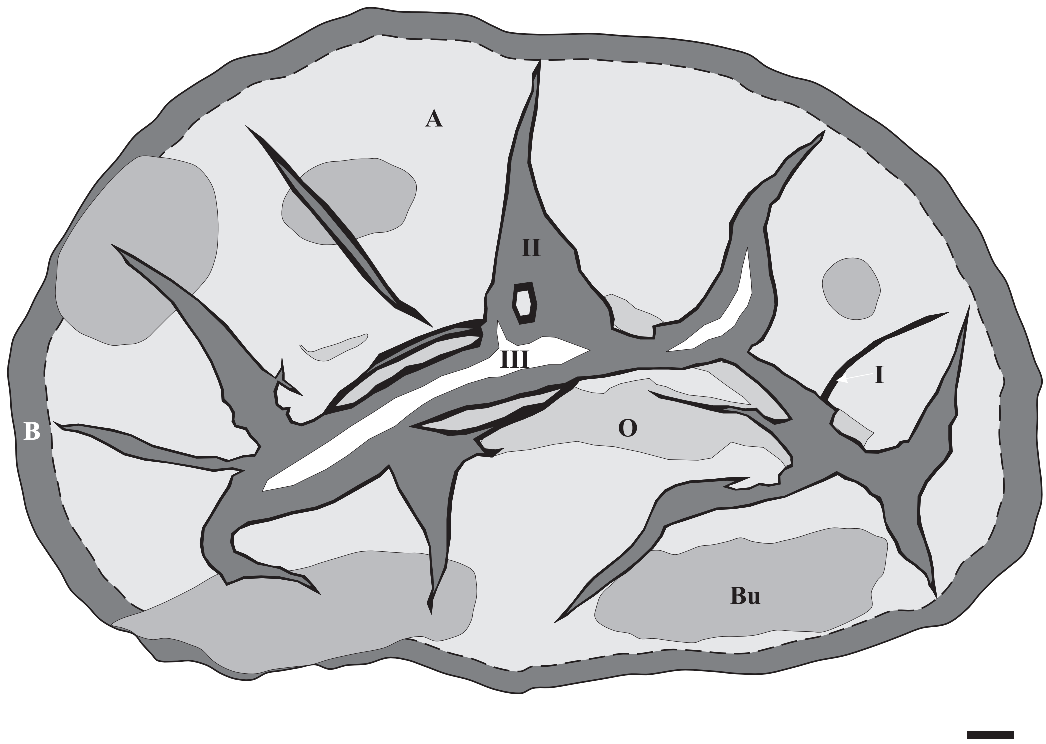

Figure 5. *Sketch of slabbed concretion in Figure 4 showing key features and cement zonation in both concretion body and septarian fracture fill. Scale bar is 1 cm. Key to stages: dominant non-ferroan calcite cement (Stage A); ferroan calcite cement (Stage B); burrows (Bu) and oyster fragment (O). Features of septarian fracture fill include dark rim of brown calcite (I), dominant infilling yellow ferroan calcite (II) and minor white ferroan calcite (III) in the core region. Note also that fractures do not penetrate to the concretion rim and are restricted to Stage A.*

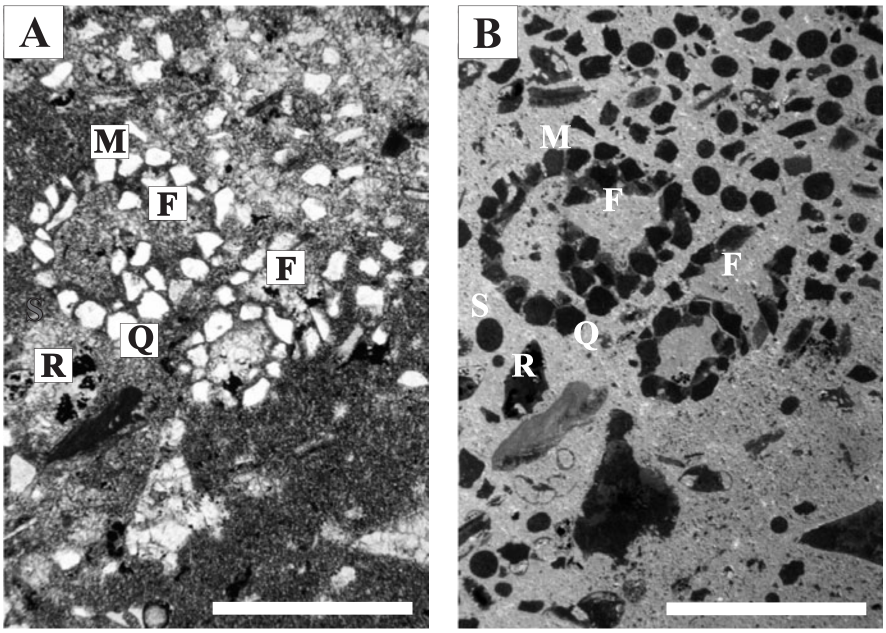

Figure 6. *Thin section photomicrographs of agglutinating foraminifera within Stage A of concretion OM17. The agglutinating foraminifera (F) (probably* Ammobaculites coprolithiformis *(Hart pers. comm., 2001)) are clearly seen under both plane polarised light (A) and* cathodoluminescence *(B). Other features of note include; very dull orange calcite spheres (S) interpreted to be replaced calcispheres, rotaliid foraminifera (R), quartz (Q), microcline (M) and the background calcite cement. Scale bar is 1 mm.*

foraminifera. Large agglutinating forms up to 1 mm across are present and have a very fine non-ferroan calcite test. Other agglutinating forms (*Haplophragmoides* sp. and *Ammobaculites* sp.) incorporated quartz grains into the test wall (Figure 6). Encrusting forms (< 300 μm) are attached to oyster and bivalve shells and rarely to calcispheres. In addition echinoid plate fragments and rare spines are present along with very rare gastropods. Wood fragments are found throughout the concretions with the cellular structure commonly replaced by pyrite.

Concretion diagenesis

The Nothe Grit Formation concretions are formed by non-ferroan and ferroan calcite, showing distinct paragenetic stages with non-ferroan calcite forming the core and majority of the concretion (Stage A) and an outer narrow rim, less than 3 cm wide composed of ferroan calcite (Stage B) (see Figure 5). Stage A cements comprise non-ferroan bright orange luminescent calcites and are either fine grained (<8 μm) equigranular euhedral microspar with abundant enfacial contacts, or equant and euhedral coarser microspar (15 - 60 μm). Ferroan calcite spheres with a dull orange CL response are very abundant and range in size from 60 to 180 μm (Figure 7). Within Stage A the spheres are composed of subhedral to euhedral calcite in the core ranging in size from 1 to 120 μm, surrounded by radially arranged bladed calcite. Within this stage the spheres have a 5 μm wide rim of non-ferroan calcite (see Figure 7).

Pyrite is present within Stage A in two forms: (1) as framboids infilling foraminifera chambers or disseminated throughout the concretion and (2) as discrete 10-150 μm sub- to euhedral crystals which are both disseminated through the concretion but are also concentrated within burrows. Glauconite both infills the chambers of some of the foraminifera and is also disseminated within the concretions. Some of the oyster shells show partial replacement by fibrous chalcedony and megaquartz cements.

Stage B is dominated by dull orange luminescent ferroan microspar (16 - 60 μm) along with minor bright orange luminescent non-ferroan fine microspar (<16 μm) cements. Zoned dolomite rhombs are present within this stage and under CL have dull orange luminescent cores (more ferroan) and bright orange (less ferroan) rims. Poikilotopic calcite cements are also present within this stage. In Stage B, the calcite spheres are composed of a mosaic of euhedral crystals increasing in size from the core to the rim of the sphere. Where the calcite spheres are present within 500 μm of either septarian veins or oyster fragments fractured by veins, they are composed of a mosaic of large ferroan calcite crystals. Pyrite is disseminated throughout Stage B and is more abundant than within Stage A.

Septarian fractures

The septarian veins within these concretions form a network of fractures radiating from the large bioclasts which form the concretion nucleus (see Figures 4 and 5). Up to four phases of cementation are present within the septarian fractures. The first phase, precipitated at the vein margins, is a brown, non-ferroan, bright orange luminescent euhedral sparry (<200 μm) calcite. This is post-dated by a brown, becoming more yellow, non-ferroan to ferroan calcite (100 μm), showing an internally zoned CL response from dull to bright orange. This is post-dated by localised clear euhedral megaquartz cements (Figure 8) which are in turn post-dated by coarsely crystalline (500 μm - 3 mm) ferroan calcite which appears light brown in hand specimen and gets coarser (3 - 6 mm) and clearer towards the centre of the fractures. Geochemical profiles based upon EDX analyses across the vein fills (Figure 9) show that the bright orange, non-ferroan calcites are Mg and Mn-rich, Fe-poor, whilst the later ferroan dull orange luminescent calcites are Fe-rich and Mn and Mg-poor. It is possible that this evolution in the composition of the cements reflects the transition from Mn to Fe reduction during post-oxic diagenesis (Hendry, 1993). In the wider fractures incompletely filled fracture porosity remains.

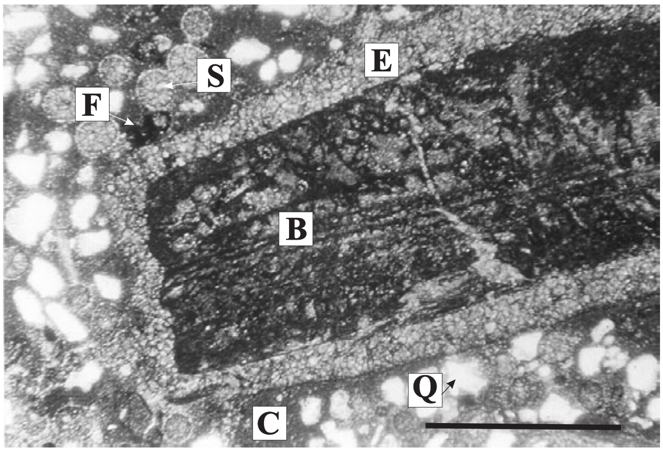

Figure 7. *Thin section (stained) photomicrograph of sample OM17-4 showing ferroan calcite spheres (S), most with very narrow non-ferroan calcite rims. Other features include quartz grains (Q), rotaliid foraminifera (F), non-ferroan calcite cement (C), neomorphosed bivalve (B) and ferroan calcite envelope (E) around replaced bivalve. Scale bar is 1 mm.*

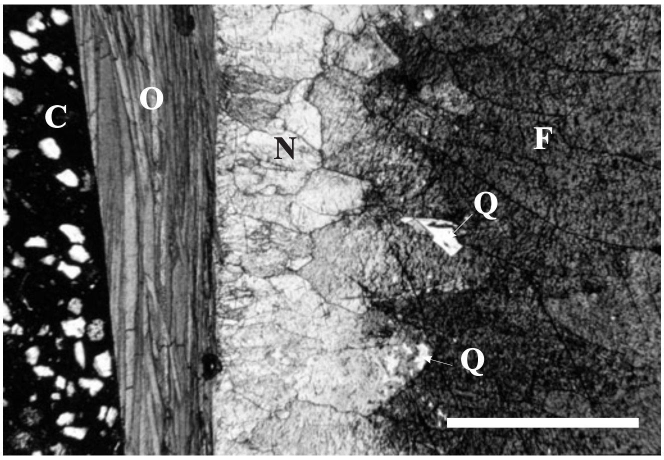

Figure 8. *Quartz cements (Q) postdating non-ferroan and ferroan calcite (N) within a septarian fracture. The quartz cements are in turn postdated by coarse ferroan calcite (F). Bounding the fracture is part of the oyster shell (O) which in turn is bounded by non-ferroan calcite cement (C) of Stage A. Scale bar is 1 mm.*

PARAGENESIS

Previous studies have interpreted the Nothe Grit Formation as representing a storm-dominated shallow marine shelf (Sun, 1989, 1990). The oysters were inverted, possibly as a result of storm winnowing, and then bored and encrusted forming a benthic island. The earliest marine diagenetic events were the precipitation of framboidal pyrite and the growth of glauconite; silicification of bioclasts is also interpreted to be early diagenetic in origin. The abundant ferroan calcite spheres are interpreted to be calcispheres replaced by ferroan calcite. They are too large to be calcitised opal-CT lepispheres, as described by Hendry and Trewin (1995). In addition, it is unlikely that they represent calcitised sponge spicules as in thin section they are always circular, hence must originally be spherical grains. The calcispheres are interpreted to have been replaced by ferroan calcite prior to the precipitation of later non-ferroan calcites. In addition both aggrading neomorphism and replacement of high Mg calcite or aragonitic bivalves by ferroan calcite is observed throughout the concretions. This early ferroan calcite was post-dated by the precipitation of the dominant non-ferroan calcite phase within Stage A. The dominant non-ferroan calcite forming Stage A is then post-dated by ferroan calcite forming the cements of Stage B.

Elevated pore fluid pressures (cf. Hounslow, 1997) led to fracturing and dilation with the first formed brittle fractures being within the lamellar ultrastructure of the bivalve at the centre of the concretion. Septarian fractures developed from the first formed horizontal fractures radiating above and below this plane, their development controlled by the extent of the oyster periphery and to a lesser extent by utilisation of major fractures bisecting the shell. The first generations of cement to form within these fractures show an evolution in composition from non-ferroan to ferroan calcite (Figure 9). This is post-dated by an interval of quartz cementation that may correspond with the quartz cements which replace some of the bioclasts. The last phase was the precipitation of the yellow to clear ferroan calcite cements, the sequence of which are comparable with brown calcite cements which commonly occur infilling vuggy porosity within ammonite chambers in Lower Jurassic concretions from Dorset (Curtis *et al.*, 2000).

The initial cementation of the concretions must have occurred at shallow burial depths as burrow outlines do not show evidence of compaction, whereas they are severely compacted in the surrounding non-concretionary sediments. However, the relative timing of the septarian fractures and related cements is more difficult to constrain. Previous studies of septarian concretions have suggested that the septaria form in response to over-

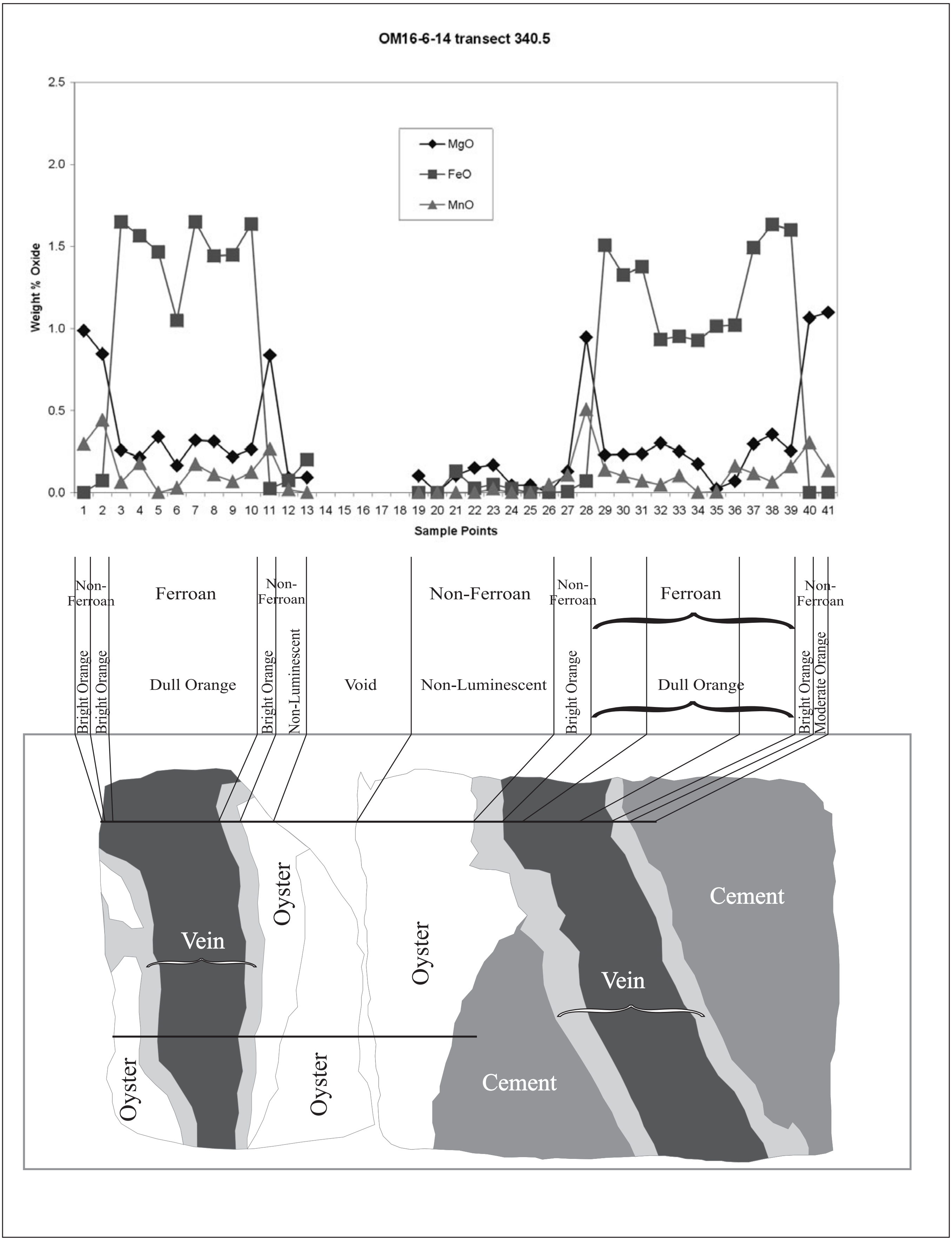

Figure 9. *Composite diagram showing main features of a thin section from OM16-6 with tie lines to a graph showing relative weight % oxide variation along a transect based upon EDX analyses. The text in the tie-lines shows the staining characteristics and cathodoluminescence response (lower). Note the elevated Fe and depressed Mg and Mn in the ferroan septarian calcite as opposed to a reverse of these trends in the bounding non-ferroan calcite whereas the oyster shell shows low Mn, Mg and Fe values.*

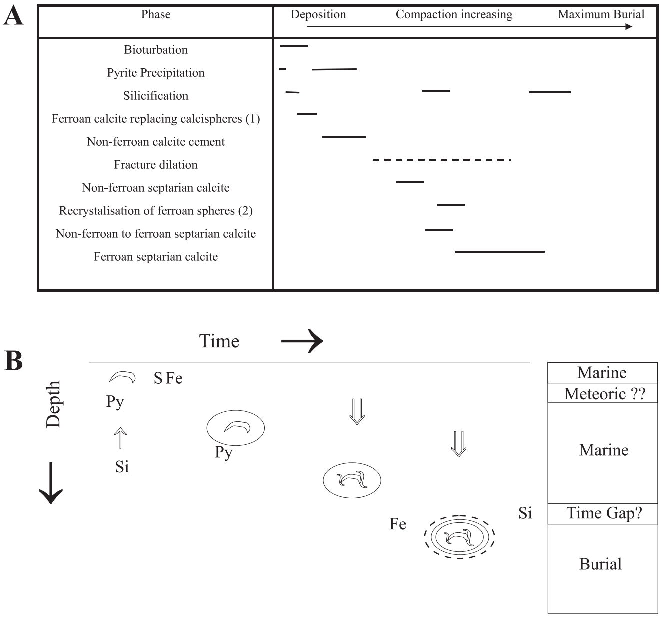

Figure 10. *(A) Detailed breakdown of paragenesis and probable timing. (B) Schematic sketch of concretion diagenesis derived from A. Right column indicates possible fluid influences. Py - pyrite, Si - silica movement, S and Fe free sulphur and iron. Increasing overburden pressure is indicated by downward arrows. Dashed line represents pre-compaction volume.*

pressuring following rapid burial (Selles-Martinez, 1996) or even potentially seismic shock at shallow depth (Pratt, 2001); ongoing stable isotope studies will resolve the timing of septarian growth and the fluid source.

ACKNOWLEDGEMENTS

Funding for David Greens PhD research programme from the CSM Trust is gratefully acknowledged. Steve Pendray and Julian Curnow are thanked for preparing the thin sections. Detailed reviews on the diagenesis by Dr Jim Hendry and the regional setting by Professor Malcolm Hart significantly improved this manuscript.

REFERENCES

ARKELL, W.J. 1933. *The Jurassic system in Great Britain*. Oxford, Clarendon Press.

ARKELL, W.J. 1936. The Corallian Beds of Dorset. *Proceedings of the Dorset Natural History and Archaeological Society*, **57**, 59-93.

ASTIN, T.R. 1986. Septarian crack formation in carbonate concretions from shales and mudstones. *Clay Minerals*, **21**, 617-631.

BJORKUM, P.A. and WALDERHAUG, O. 1990. Lateral extent of calcite-cemented zones in shallow-marine sandstones. In: BULLER, A.T., BERG, E., HJELMLAND, O., KLEPPE, J., TORSAETER, O. and AASEN, J.O., (eds), *North Sea Oil and Gas Reservoirs II*. Graham and Trotman, London, 331-336.

COE, A.L. 1995. A comparison of the Oxfordian succession of Dorset, Oxfordshire and Yorkshire. In: TAYLOR, P.D., (Ed.), *Field geology of the British Jurassic.* Geological Society, London, 151-172.

CURTIS, C.D., COPE, J.C.W. and MACQUAKER, J.H.S. 2000. 'Instantaneous' sedimentation, early microbial sediment strengthening and a lengthy record of chemical diagenesis preserved in Lower Jurassic ammonitiferous concretions from Dorset. *Journal of the Geological Society, London*, **157**, 165-172.

DE WET, C.B. 1987. Deposition and diagenesis in an extensional basin: the Corallian Formation (Jurassic) near Oxford, England. In: MARSHALL, J.D., (Ed.), *Diagenesis of sedimentary sequences*. Geological Society, London, Special Publication, **36**, 339-353.

DICKSON, J.A.D. 1966. Carbonate identification and genesis revealed by staining. *Journal of Sedimentary Petrology*, **36**, 491-505.

DICKSON, J.A.D. and BARBER, C. 1976. Petrography, chemistry and origin of early diagenetic concretions in the Lower Carboniferous of the Isle of Man. *Sedimentology*, **23**, 189-211.

FÜRSICH, F.T. 1975. Trace fossils as environmental indicators in the Corallian of England and Normandy. *Lethaia*, **8**, 151-172.

HENDRY, J.P. 1993. Calcite cementation during bacterial manganese, iron and sulphate reduction in Jurassic shallow marine carbonates. *Sedimentology*, **40**, 87-106.

HENDRY, J.P. and TREWIN, N.H. 1995. Authigenic quartz microfabrics in Cretaceous turbidites: evidence for silica transformation processes in sandstones. *Journal of Sedimentary Research*, **A65**, 380-392.

HESSELBO, S.P. and PALMER, T.J. 1992. Reworked early diagenetic concretions and the bioerosional origin of a regional discontinuity within British Jurassic marine mudstones. *Sedimentology*, **39**, 1045-1065.

HOUNSLOW, M.W. 1997. Significance of localized pore pressures to the genesis of septarian concretions. *Sedimentology*, **44**, 1133-1147.

HUDSON, J.D., COLEMAN, M.L., BARREIRO, B.A. and HOLLINGWORTH, N.T.J. 2001. Septarian concretions from the Oxford Clay (Jurassic, England, UK): involvement of original marine and multiple external pore fluids. *Sedimentology*, **48**, 507-531.

NEWELL, A.J. 2000. Fault activity and sedimentation in a marine rift basin (Upper Jurassic, Wessex Basin, UK). *Journal of the Geological Society, London*, **157**, 83-92.

OXFORD, M.J., HART, M.B. and WATKINSON, M.P. 2000. Micropalaeontological investigations of the Oxford Clay - Corallian succession of the Dorset coast. *Geoscience in south-west England*, **10**, 9-13.

PRATT, B.R. 2001. Septarian concretions: internal cracking caused by synsedimentary earthquakes. *Sedimentology*, **48**, 189-213.

RAISWELL, R. 1971. The growth of Cambrian and Liassic concretions. *Sedimentology*, **17**, 147-171.

RAISWELL, R. 1987. Non-steady state microbial diagenesis and the origin of concretions and nodular limestones. In: MARSHALL, J.D., (Ed.), *Diagenesis of sedimentary sequences*. Geological Society, London, Special Publication, **36**, 41-54.

SCOTCHMAN, I.C. 1993. Diagenetic pore fluid evolution in the Kimmeridge Clay Formation: from concretions to sandstone cements. In: MANNING, D.C., HALL, P.L., and HUGHES, C.R., (eds), *Geochemistry of clay-pore fluid interactions*. Chapman and Hall, London, 127-159.

SELLES-MARTINEZ, J. 1996. Concretion morphology, classification and genesis. *Earth Science Reviews*, **41**, 177-210.

SUN, S.Q. 1989. A new interpretation of the Corallian (Upper Jurassic) cycles of the Dorset coast, southern England. *Geological Journal*, **24**, 139-158.

SUN, S.Q. 1990. Facies-related diagenesis in a cyclic shallow marine sequence: the Corallian Group (Upper Jurassic) of the Dorset coast, southern England. *Journal of Sedimentary Petrology*, **60**, 42-52.

TALBOT, M.R. 1973. Major sedimentary cycles in the Corallian Beds (Oxfordian) of southern England. *Palaeogeography, Palaeoclimatology, Palaeoecology*, **14**, 293-317.

WALDERHAUG, O., BJORKUM, P.A. and NORDGAS BOLAS, H.M. 1989. Correlation of calcite-cemented layers in shallow-marine sandstones of the Fensfjord Formation in the Brage Field. In: COLLINSON, J.D., (Ed.), *Correlation in hydrocarbon exploration*. Graham and Trotman, London, 367-375.

WILKINSON, M. 1992. Concretionary cements in Jurassic sandstones, Isle of Eigg, Inner Hebrides. In: PARNELL, J., (Ed.), *Basins on the Atlantic seaboard: Petroleum geology, sedimentology and basin evolution*. Geological Society, London, Special Publication, **62**, 145-154.

WILKINSON, M. 1993. Concretions of the Valtos Sandstone Formation of Skye: geochemical indicators of palaeohydrology. *Journal of the Geological Society, London*, **150**, 57-66.

WILSON, R.C.L. 1968. Upper Oxfordian palaeogeography of southern England. *Palaeogeography, Palaeoclimatology, Palaeoecology*, **4**, 5-28.

WOLFF, G.A., RUKIN, N. and MARSHALL, J.D. 1992. Geochemistry of an early diagenetic concretion from the Birchi Bed (Lower Lias, W. Dorset, UK). *Organic Geochemistry*, **19**, 431-444.

WRIGHT, J.K. 1986. A new look at the stratigraphy and ammonite fauna of the Corallian Group (Oxfordian) of south Dorset. *Proceedings of the Geologists' Association*, **97**, 1-21.